

RESEARCH

Open Access



Analysis of Interface Properties Between TRC and Concrete Under Chloride Attack Based on Fracture Energy

Shichang Li¹, Shiping Yin^{1,2*}  and Yu Gao¹

Abstract

As a type of cement-based composite reinforcement material, textile reinforced concrete (TRC) has the advantages of corrosion resistance, high bearing capacity and good crack limit performance. Its bonding performance with the existing concrete interface is the key factor affecting the reinforcement effect. To study the interfacial adhesion between TRC and existing concrete, the sodium chloride concentration, the frequency and number of dry and wet cycles, the bonding length of the TRC reinforcement layer and the type of reinforcement were analysed by a double-sided shear test, XRD (X-ray diffraction) and SEM (scanning electron microscope) micro-test techniques. The influence of other factors on the interfacial bonding properties was further elaborated based on the theory of fracture energy. The results show that interface damage under chloride attack was mainly divided into three typical interface failure modes. By increasing the concentration of sodium chloride, reducing the frequency of dry and wet cycles and increasing the number of dry and wet cycles, the interface microstructure damage could be aggravated. Using cast-in-place reinforcement and increasing the bonding length could enhance the bonding performance of the interface.

Keywords: TRC, existing concrete, bonding performance, chloride corrosion, microstructure, fracture energy

1 Introduction

Chloride salt erosion and periodic wet and dry cycles in the marine environment are one of the main reasons for the decrease in service life of reinforced concrete structures in ports and sea areas, and they also threaten the overall security of the structures in several cases. Reinforcement is an effective way to extend the service life and enhance the safety of the structure. FRP (fibre reinforced polymer) sheets are widely used in structural reinforcement because of their good performance; however, the use of epoxy resin as the matrix of FRP makes it unsuitable for construction in humid or low-temperature environments. Cement-based materials can not only

overcome the shortcomings of the resin matrix but also provide a new alkaline environment for the structure to be repaired and strengthened (Triantafillou et al. 2006; Bournas et al. 2007). Textile reinforced concrete (TRC) is a type of composite material made of a textile and high-performance mortar (Barhum et al. 2012; Hegger et al. 2006), which has excellent crack-limiting performance, high tensile strength and corrosion resistance. As a reinforcement layer, it has good coordination and compatibility with the existing concrete and can make up for the limitations of FRP application (Peled 2007; Yin et al. 2014, 2015). In addition, the core concepts of textile-reinforced mortar (TRM) (Triantafillou et al. 2006) and fabric-reinforced cement matrix (FRCM) (Ascione et al. 2015) are the same as TRC and have similar superior performance.

At present, the research on the interface performance of new and old concrete has had more research results. (Diab et al. 2017) found that the increase in compressive strength of cast-in-place concrete and the increase in the

*Correspondence: yinshiping2821@163.com

¹ Jiangsu Key Laboratory of Environmental Impact and Structural Safety in Engineering, School of Mechanics & Civil Engineering, China University of Mining and Technology, Xuzhou 221116, Jiangsu, China
Full list of author information is available at the end of the article
Journal information: ISSN 1976-0485 / eISSN 2234-1315

roughness of existing concrete will increase the bond strength of new and old concrete. (Momayez et al. 2005) found that the incorporation of silica fume in concrete and the improvement of interface roughness can improve the bonding properties of new and old concrete. (Mousa 2015) studied the influence factors of interface bond strength of new and old concrete, mainly including: selection of interface agent; interface bond form; interface roughness; type of reinforced concrete material; interface permeability, etc. However, there are few studies on the interfacial bond between TRC and existing concrete. The bond performance of the interface between TRC and existing concrete has an important influence on the performance of existing concrete structures strengthened by TRC, which is the basic factor for TRC to be applied in engineering practice. At present, some scholars have carried out relevant studies on the bond performance of the interface between TRC and existing concrete in a conventional environment. (Ascione et al. 2015) analysed the interface failure modes of the FRCM reinforced layer and existing concrete and the corresponding bond-slip curve. (Ortlepp et al. 2006) found that the strain distribution of TRC thin plates was not continuous during the interface cracking process. Based on this outcome, the development process of cracks in the bonding failure was elaborated, and the basic bond-slip theory of the TRC strengthened interface was proposed. Furthermore, (D'Ambrisi et al. 2012, 2013) verified the bond-slip curve between FRCM and existing concrete through a double-side shear test, corrected the bond-slip model, and verified the effectiveness of FRCM reinforcement from the perspective of fracture energy. In addition, there are few studies on the bond between TRC and existing concrete under an erosion environment. (Yin et al. 2018) deduced the formula for calculating the bond between TRC and existing concrete under chloride erosion based on the plastic limit analysis theory and the interface model of new and old concrete. (Yin et al. 2018) studied the influence of precracking of the TRC reinforcement layer, existing concrete strength, interface form, chopped fibre and freeze–thaw cycle times on the bonding performance of TRC and existing concrete interface under a chloride freeze–thaw cycle through a double-side shear test and confirmed the application value of TRC in the reinforcement and repair of existing concrete structure under a chloride freeze–thaw environment.

The above studies indicate that current research has mainly focused on the conventional environment, and the bond performance mechanism of the existing concrete interface in TRC reinforcement under an erosion environment is not clear; thus, it is necessary to carry out research in this regard. Therefore, this paper analyses the chloride salt erosion environment of sodium chloride concentration,

dry and wet cycle frequency and type, TRC reinforcement layer bond length and reinforcement effect on the performance of the TRC and existing concrete interface bonding, and through the interface fracture further verifies the analysis.

2 Test Conditions

2.1 Test Materials

Specific information of C40 concrete raw material: 42.5R ordinary Portland cement, crushed stone with particle sizes of 5–10 mm, medium sand, tap water and polycarboxylic acid as a high-efficiency air intake and water-reducing agent are selected. The proportions are shown in Table 1.

The textile is made of carbon fibre bundles and glass fibre bundles in the radial and weft directions, respectively. The mesh size is 10 mm × 10 mm, and the thickness is approximately 2 mm. To improve the bonding performance between the textile and fine-grained concrete, impregnated epoxy resin and bonding sand was used to treat the textile. The performance indexes of the textile are shown in Table 2.

Fine-grained concrete has good mobility and performance for self-compacting concrete and can work together with the textile. Specific information of raw materials for fine-grained concrete: 52.5 R-grade ordinary Portland cement, fly ash, polycarboxylic acid as a high-efficiency air intake and water-reducing agent, quartz sand with particle size of 0–0.6 mm and quartz sand with particle size of 0.6–1.2 mm, silica fume and tap water. The proportions are shown in Table 3.

2.2 Sample Design and Fabrication

Two TRC reinforcements for existing concrete methods are designed in the test: cast-in-place reinforcement and prefabricated TRC-paste reinforcement, as shown in Fig. 1. Cast-in-place reinforcement: (1) After the interface treatment, the formwork on both sides of the surface of the existing concrete are supported by formwork. The length of the formwork is selected according to the design value. The width and thickness of the formwork is 100 mm × 6 mm, and the fine-grained concrete is applied and smoothed. (2) The textile is stretched onto the wooden formwork; (3) an air nail gun is used to nail a 6-mm thick wooden strip around the formwork, and then the fine-grained concrete is applied flush with the surface of the wood strip. However, during the actual construction, the

Table 1 Mix proportion of existing concrete (kg/m³).

Type of concrete	Cement	Water	Medium sand	Gravel	Water reducing agent
C40	415/42.5R	161	643	1181	2.85

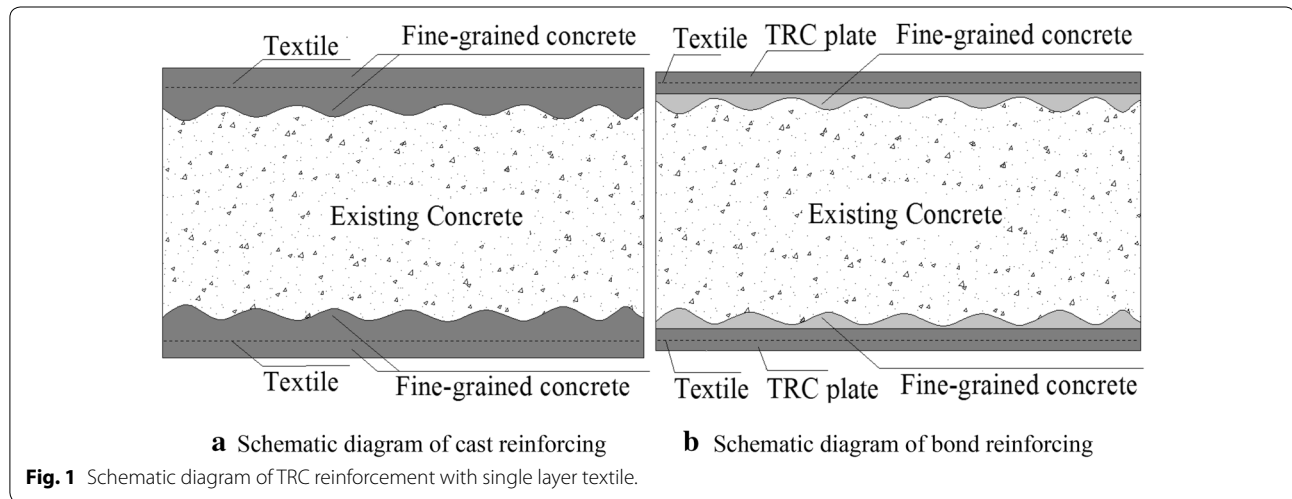
Table 2 Mechanical properties of textile.

Fibre type	Number of fibres per bundle	Tensile strength of monofilament fibres/MPa	Elastic modulus of monofilament fibre/GPa	Breaking elongation of monofilament fibres/%	Fibre bundle linear density/tex	Bundle density/(g/cm ³)
T700S	12k	4660	231	2	801	1.78
E-glass	4k	3200	65	4.5	600	2.58

Annotation: 1Tex = 1 g/km.

Table 3 Mix proportion of fine-grained concrete (kg/m³).

Cement	Fly ash	Silica fume	Water	Fine sand	Coarse sand	Water reducing agent
475/52.5R	168	35	262	460	920	9.1



TRC reinforcement is not easily adopted in some special positions with the cast-in-place method, so the prefabricated TRC-plate reinforcement is adopted: (1) TRC plates of different lengths are made, of which the width and thickness are 100 mm × 12 mm; (2) after the interface treatment of the existing concrete surface, the fine-grained concrete is evenly spread on the surface at 2–3 mm; (3) the prepared TRC plate is placed where fine-grained concrete is laid; (4) to ensure bonding performance between the TRC slab and the existing concrete, heavy objects are placed on the pasted and aligned TRC plates, after 3 days of indoor maintenance, it was placed in a standard curing room for 25 days.

2.3 Chloride Erosion and Loading Device

The test was carried out under the environment of indoor nature, its temperature at 17 °C and relative humidity at 70%. When the dry and wet circulation frequency is 1 day/time, the specimen is completely soaked in sodium chloride solution at room temperature for 12 h, and then

the sodium chloride solution is removed to make the specimen dry in the room for 12 h. When the dry and wet cycle frequency is 2 days/time, the specimen is completely soaked in sodium chloride solution for 24 h and then dried in the room for 24 h. In addition, the effects of different concentrations of sodium chloride solution and the number of different wet and dry cycles on the test results were also investigated.

The double-side shear test was used to study the interface performance between the TRC and existing concrete. By this test method, the failure mode of the interface between TRC reinforcement layer and existing concrete can be obtained. The test by loading the pressure above the existing concrete, the maximum pressure value was obtained when the TRC and existing concrete members are destroyed at the same time or one of them reaches damage. Among them, a pressure sensor is placed on the steel plate loaded on the top of the test piece to collect the vertical load of the test piece. In addition, after previous exploration experiments, it was found

that the absolute displacement of the outer TRC plate relative to the ground was almost zero (about a few thousandths of a millimeter) for this specimen. Therefore, in the subsequent test process, the absolute displacement of the existing concrete was directly measured with a displacement meter to indicate the slip between the TRC plate and the existing concrete. The displacement meter is fixed by the magnetic stand on the ground, and its test end is placed in the lateral middle position of the existing concrete. The test machine adopts the displacement control mode to carry out forward monotonic loading. The loading rate is 0.5 mm/min, and the loading diagram is shown in Fig. 2. In the static test, the shear load and the interface slip between the TRC and the existing concrete were collected by a GBD3816 static strain Testing and analysis system produced by Jiangsu Donghua Testing Technology Co., Ltd at the same interval of 10 s.

2.4 Microscopic Testing Technology

2.4.1 X-ray Diffraction (XRD) Test

This experiment was carried out in Modern Analysis and Calculation Center. The samples were taken from the specimens after the double-sided shear test, and the sampling location was the fine-grained concrete part in the interface area between TRC and existing concrete. The block sample was first cleaned of dust in anhydrous alcohol, then grinded in a mortar, and the powder sample was obtained through a 325 mesh sieve. The powder sample was placed on the X-ray diffractometer and scanned to obtain the XRD pattern.

2.4.2 Scanning Electron Microscope (SEM) Observation Test

This experiment was also carried out in Modern Analysis and Calculation Center. The samples were taken from the specimens after the double-sided shear test, and the sampling location was the fine-grained concrete part in the interface area between TRC and existing concrete. The sample size shall not be more than 10 mm × 10 mm.

The sample terminates the hydration of concrete in anhydrous alcohol and cleans the surface of floating ash. The gold-treated specimens were observed in a high-vacuum Quanta250 scanning electron microscope for surface porosity, hydration products, and cracks.

2.5 Test Group

A total of 33 specimens were made according to different research factors. To reduce the experimental error, three specimens were made for each group in the experiment. The specimens are numbered in the form of X-Y-Z. Where X is L, which represents the bonding length of the reinforcement layer, and L100, L200, and L300 respectively indicate that the bonding length of the reinforcement layer is 100 mm, 200 mm, and 300 mm; Y is R, stands for reinforcement form, where R_p stands for prefabricated-paste and R_c stands for cast-in-place; Z is numbered 1–8, which represents different wet and dry cycle environment of chlorine salts. The specific information contained in different Numbers is shown in Table 4. For example, L200-R_p-1 represents that the bond length of TRC reinforcement is 200 mm, the reinforcement form is prefabricated and pasted, the concentration of sodium

Table 4 Specimen information under different environments of chloride salt erosion.

Serial number	Concentration of sodium chloride solution/%	Dry and wet cycles	Cycle frequency
1	5	120	1 day/time
2	–	–	–
3	5	–	–
4	2.5	120	1 day/time
5	7.5	120	1 day/time
6	5	90	1 day/time
7	5	150	1 day/time
8	5	120	2 day/time

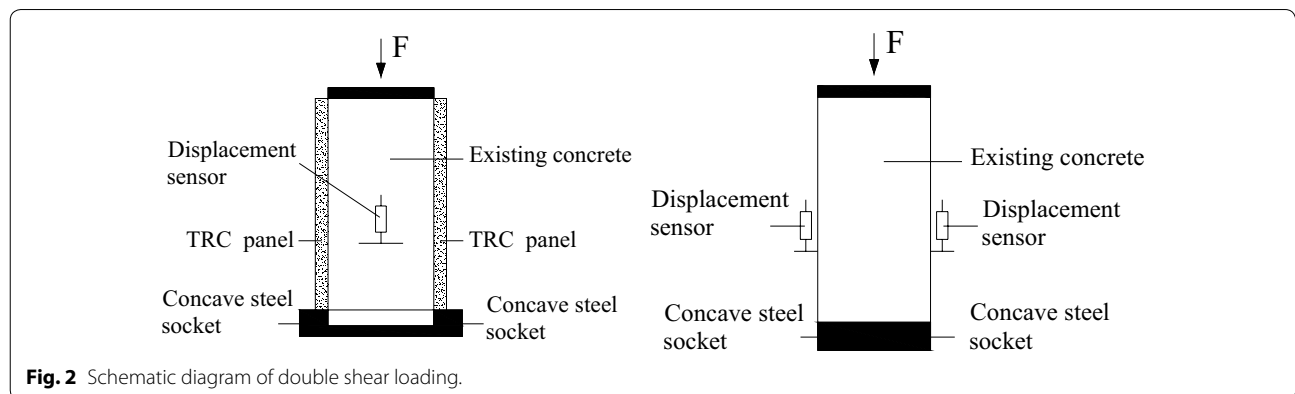


Fig. 2 Schematic diagram of double shear loading.

chloride solution is 5%, the number of dry and wet cycles is 120, and the cycle frequency is 1 day/time. (Remarks: all the existing concrete surface is treated by manual roughening and the depth of sand filling is 2–4 mm).

3 Test Results and Analysis

According to the double-sided shear test, the data of maximum interface shear load and maximum interface deformation slip under different research factors are summarized in Table 5.

3.1 Interface Failure Mode

As shown in Fig. 3a–c, three typical failure modes of TRC strengthened existing concrete specimens under chloride erosion are summarized by analysing the macroscopic characteristics of the interface fracture process and morphology. Namely, double-sided shear failure, TRC layered

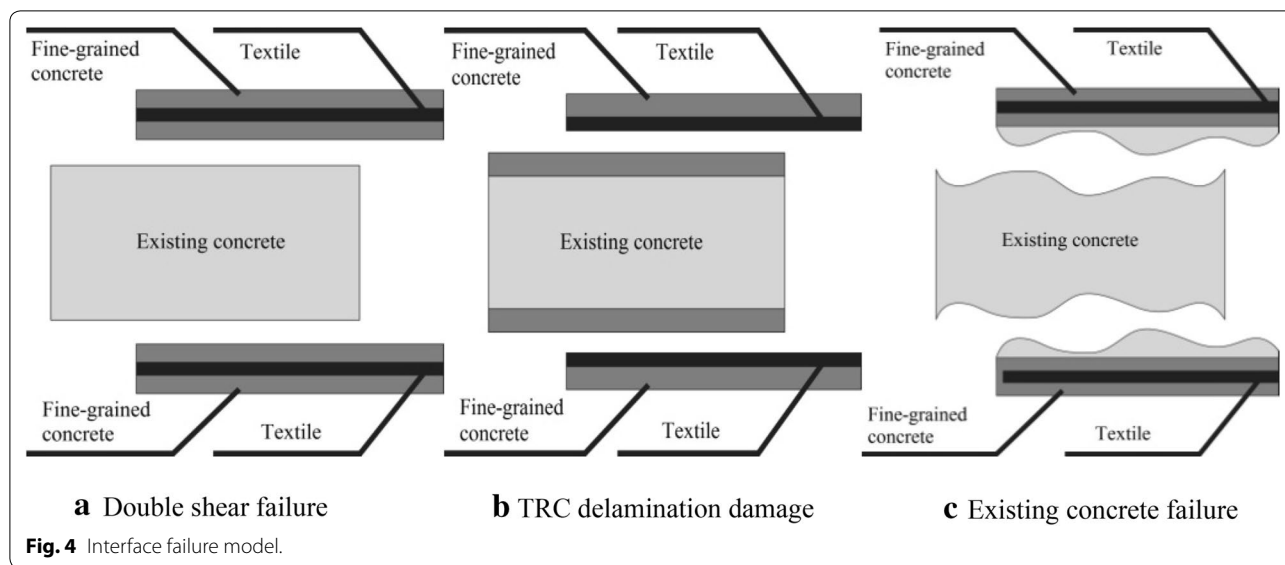
failure and existing concrete failure were concluded. The main reason was that the interface bond mechanism changed under different working conditions.

The first type of interface failure mode was double shear failure, as shown in Fig. 4a. As the vertical load force approached the limit load, the lateral deformation of the TRC plate occurred, the TRC and existing concrete interface cracked at the bottom, cracks along the interface rapidly extended from bottom to top and throughout the entire reinforcement interface, and the TRC plate was separated from the existing concrete at the interface. The second interface failure mode was TRC delamination damage, as shown in Fig. 4b. When the length of the reinforcement layer increased, the experimental phenomenon in the early stage is basically the same as that in the first type of interface failure. When the vertical load achieved the maximum interfacial bond, the textile and

Table 5 Specimen bond properties and failure forms.

Serial number	Maximum interfacial shear load F/kN		Maximum interfacial deformation and sliding S_f/mm		Ultimate shear strength τ_f/MPa	Failure pattern
	Average	Standard deviation	Average	Standard deviation		
L200-R _p -1	61.10	1.849	0.480	0.02944	1.526	Double side shear
L200-R _p -2	106.30	1.791	0.555	0.02160	2.657	Double side shear
L200-R _p -3	96.80	1.846	0.605	0.01472	2.420	Double side shear
L200-R _p -4	65.85	1.102	0.365	0.02858	1.646	Double side shear
L200-R _p -5	55.13	2.180	0.451	0.02531	1.378	Double side shear
L200-R _p -6	74.58	1.577	0.530	0.01780	1.864	Double side shear
L200-R _p -7	51.10	1.105	0.305	0.01225	1.278	Double side shear
L200-R _p -8	45.65	1.674	0.530	0.00816	1.141	Double side shear
L300-R _p -1	99.05	2.245	0.905	0.03629	1.651	TRC layered
L100-R _p -1	39.20	2.177	0.265	0.02041	1.960	Double side shear
L200-R _c -1	158.73	1.698	0.415	0.01551	3.968	Existing concrete failure





the fine-grained concrete matrix in the TRC reinforcement layer at the base began to delaminate, cracks along the textile extended upward, and layered failure occurred. The third type of interface failure mode was the failure of existing concrete, as shown in Fig. 4c. When using cast-in-place reinforcement, the experimental phenomenon in the early stage is basically the same as that in the first type of interface failure. When the vertical load achieved the maximum interfacial bond, cracks extended from bottom to top in the existing concrete and penetrated the entire interface, and the specimens lost bearing capacity.

In summary, in the chloride erosion environment, the failure modes of most specimens occurred at the interface between the TRC plate and existing concrete; that is, double-sided shear failure mode occurred. However, by increasing the length of the TRC reinforcement layer, the bonding strength of the interface could be enhanced, and TRC delamination failure occurred at the interface. By changing the form of TRC reinforcement from prefabricated paste to cast-in-place reinforcement, the bonding performance of the interface could be improved, and the failure of the interface occurred at the existing concrete. Therefore, the interface failure mode can be changed by properly changing the reinforcement conditions so that the best interface bonding performance can be achieved by TRC reinforcement of existing concrete.

3.2 Interface Failure Mechanism

The failure mechanism of the interface between the TRC and existing concrete in a chloride erosion environment was analysed from a micro-perspective. Analytical samples was the fine-grained concrete part in the interface area between TRC and existing concrete, and XRD and

SEM analyses of the material composition and structure of the interface microstructure changes were conducted to explore the interface bonding failure mechanism under chloride salt erosion.

As shown in Fig. 5a, after immersion in the chloride salt solution, the maximum interfacial shear load is slightly reduced compared with the conventional environment. According to the analysis in Fig. 6a, b, hydration products on both sides of the crack are connected to each other in the conventional environment, the pore filling in the interface transition zone is basically complete, and the entire microstructure is relatively dense. However, the microstructure of the interface soaked in chloride solution is relatively complex, with a small number of micro-cracks. As shown in Fig. 5b, as the concentration of chloride salt increases, the maximum interface shear load is gradually less. As seen in Fig. 6c, when the concentration of sodium chloride is increased, the interface microstructure is relatively loose, there are many pores not filled with hydration products, and many needle cluster hydration products are generated on the structure surface and between pores. As shown in Fig. 5c, d, when the number of dry and wet cycles of chloride salt increases, the maximum interfacial shear load decreases continuously, and the dry-wet cycle frequency has a greater influence on the maximum interfacial shear load. When the single cycle time increases, the maximum interface shear load decreases significantly. It can be seen in Fig. 6d, e that when the number of dry and wet cycles of chlorine salts increases and the single cycle time increases, the interface microstructure of the TRC and existing concrete is damaged. There are many pores in the microstructure, and there are acicular and short

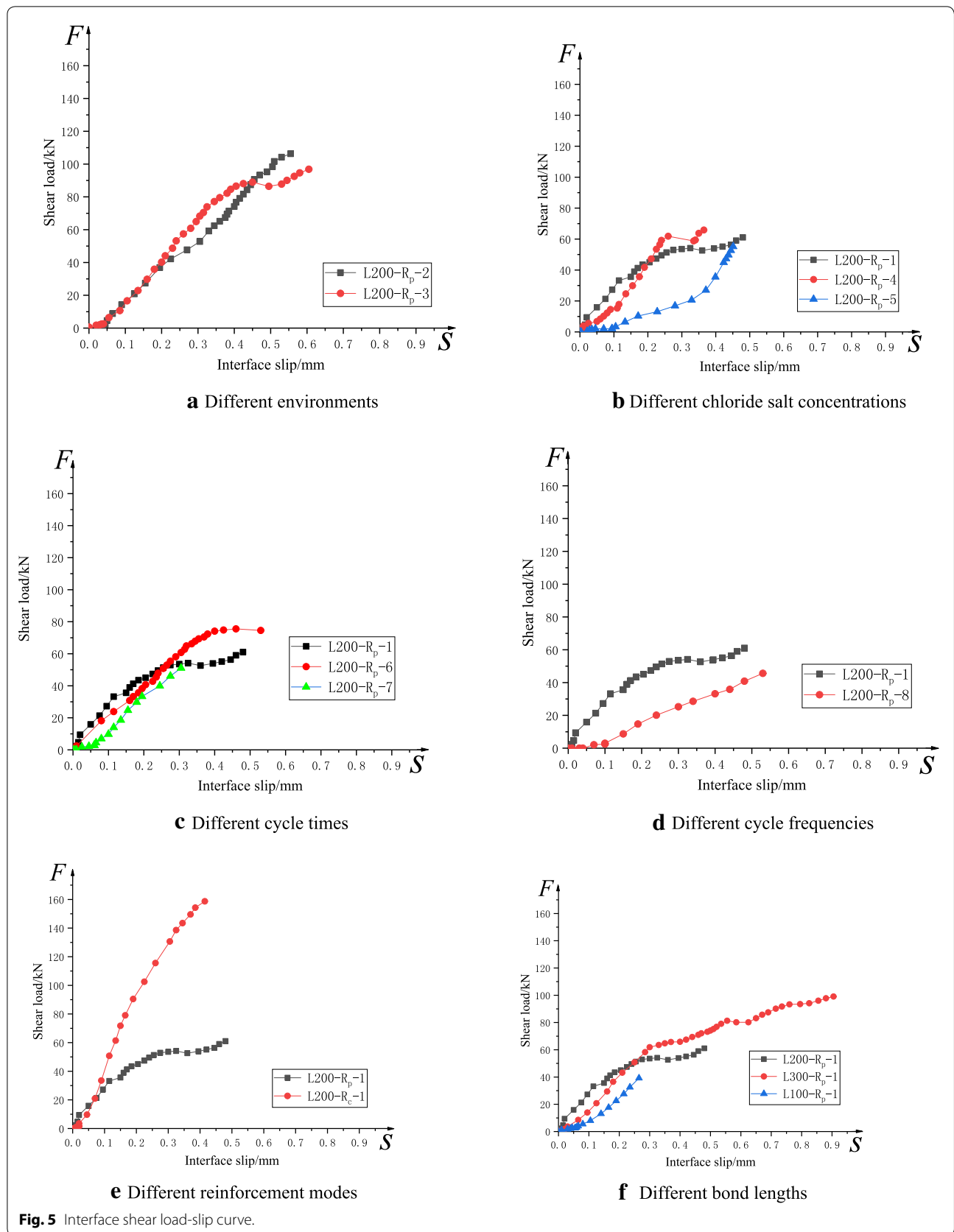


Fig. 5 Interface shear load-slip curve.

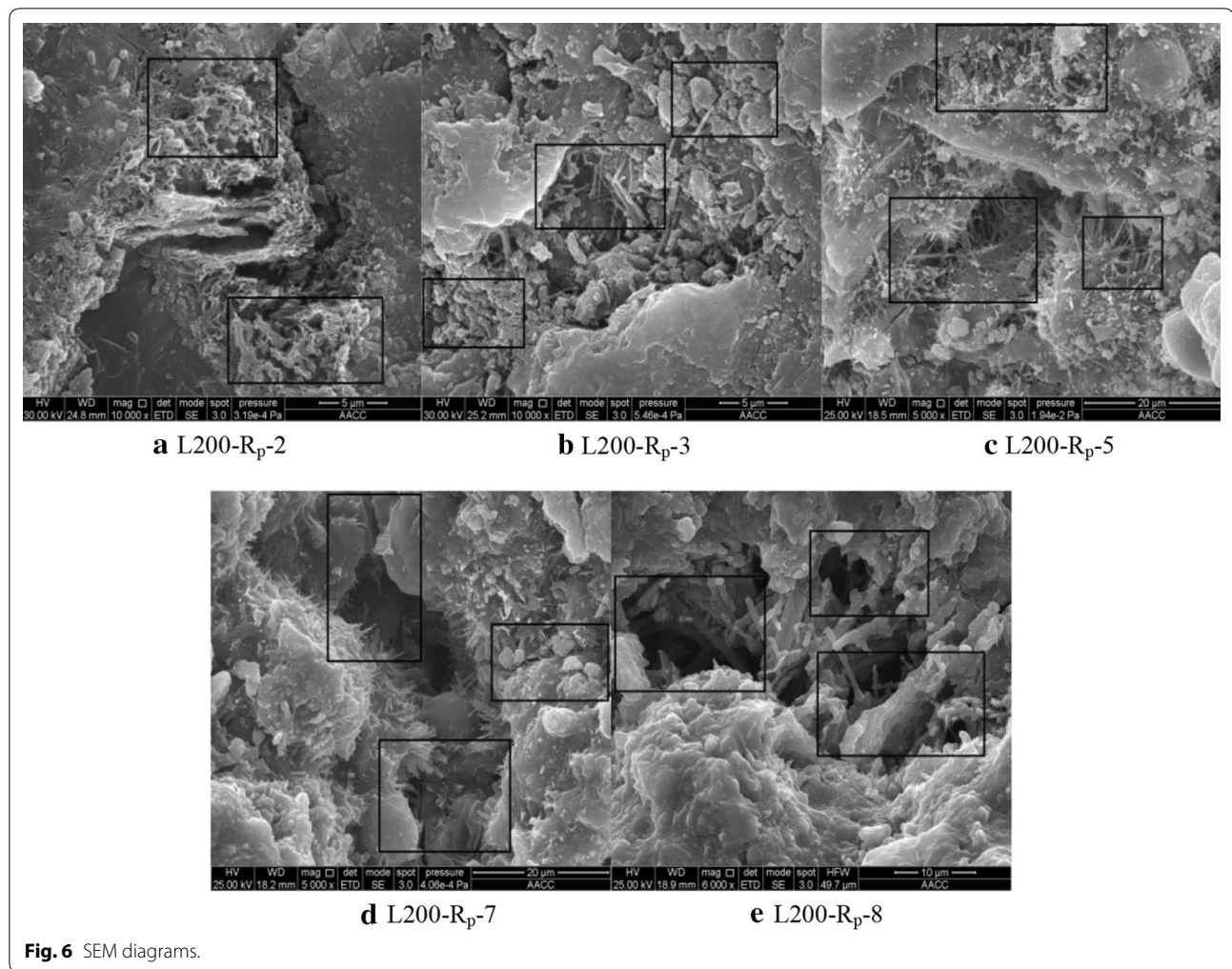


Fig. 6 SEM diagrams.

columnar hydration products in the pores, resulting in obvious cracks.

As shown in Fig. 5e, f when the cast-in-place reinforcement is used or the bond length of the reinforcement layer is increased, the maximum shear load at the interface is correspondingly increased. It shows that the interface between the TRC plate and the existing concrete can be analyzed from three forces: mechanical bite force, van der Waals force and chemical force (Li et al. 2001). Mechanical biting force means that the burrs of the fine-grained concrete hydration product C-S-H gel are radiated into the capillary pores of the existing concrete. Moreover, since the existing concrete has a relatively short age, and the internal unhydrated portion or the incompletely hydrated portion grows and grows up in the new concrete, the mechanical biting force due to the radiation effect of the hydration product is considerable. Van der Waals force is mainly caused by the molecular interaction between crystals and crystals in the interface

material and between the crystal and the aggregate. When TRC is used to reinforce the existing concrete, the spacing between the two crystals is large, so the bonding force generated by van der Waals force is still relatively small. The chemical force is mainly derived from the reaction of the cement component of fine-grained concrete with the unhydrated part of the existing concrete and the hydrate. Therefore, the main reasons for the decrease of interfacial adhesion were analysed: (1) Under the action of dry and wet circulation, the absorption of concrete capillary pores accelerated the diffusion rate of the chloride and accelerate the accumulation of chloride ions at the concrete interface (Lu et al. 2007). When the water evaporates and loses water, the salt solution in the pores becomes crystal due to oversaturation, resulting in a crystallization expansion pressure. And because of the shrinkage and swelling effect, the deterioration of concrete performance is aggravated, and the drying transition zone in the microstructure has obvious cracks.

The mechanical biting force formed by interlacing and coexisting with the existing concrete after hardening of the cement slurry in the interface region is reduced; (2) Under the chloride erosion environment, due to concrete hydration and interfacial adhesion bubbles and other reasons, the structure of the interfacial area was loose and porous, and the distance between molecules was large, which reduced the Van der Waals force in the interfacial area; (3) As shown in Fig. 7a, after chloride salt erosion the main interfacial phases except for the initial three main phases, the initial product exhibited less typical erosion product Friedel's salt ($C_3A \cdot CaCl_2 \cdot 10H_2O$) (Marinescu et al. 2012; Balonis et al. 2010; Elakneswaran et al. 2009). This is because with the continuous intrusion of the chloride salt solution, the complexity of the hydration product in the interface region is increased, and the chemical interaction of the interface region is lowered. In addition, according to the analysis in Fig. 7b–d, the content of Friedel's salt in different chloride concentration, cycle times and cycle frequency of chloride salt dry and wet cycle is less, and there is no significant change. It shows that the damage of interface microstructure is not mainly caused by chemical corrosion.

In summary, under the action of chloride erosion, a complex chemical salt corrosion reaction is generated between the TRC and the concrete at the existing concrete interface. The cement slurry C-S-H gel can react with chloride ions in the erosion medium to produce the new microscopic substance Friedel's salt. In addition, in the conventional environment, the microstructure of the interface between TRC and existing concrete is relatively dense, the interface bond strength is high, and the overall performance is excellent. In the chloride erosion environment, increasing the concentration of chloride solution, reducing the cycle frequency and increasing the number of dry–wet cycles affects the interface microstructure between the TRC and existing concrete, resulting in damage and degradation of the interface microstructure, leading to a decline in the overall performance of the structure.

3.3 Interfacial Fracture Energy Analysis of Bond Properties

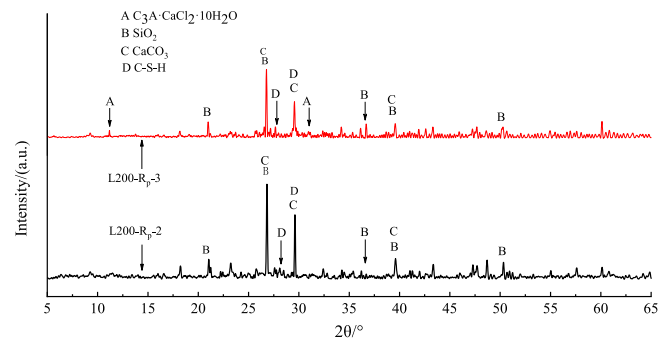
The interfacial fracture energy is the average energy consumed by the crack fracture propagation per unit area when the bonding fracture occurs, which can well reflect the fracture characteristics of the material and determine the extent of the fracture propagation after the bonding slip and the failure of the interface (Yang et al. 2016). (Detassis et al. 1996) explored the interface fracture energy through experiments and concluded that the interface failure process could be effectively delayed when the interface fracture energy parameter increased. In summary, the interfacial fracture energy is closely

related to the fracture characteristics of materials, which can be used to characterize the bonding performance of TRC and existing concrete against interfacial fracture in a double-side shear test. Its expression is as follows:

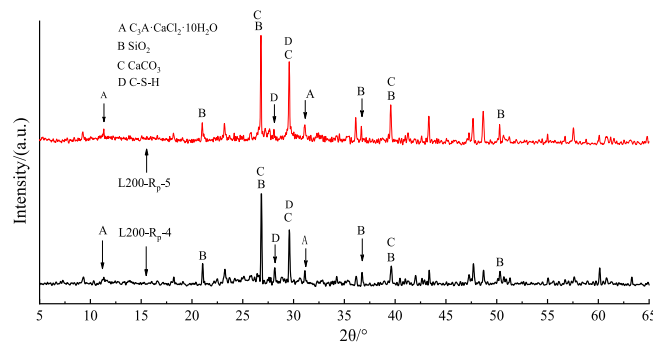
$$G_f = \int_0^s \tau(s) ds \quad (1)$$

where G_f is the interfacial fracture energy of the system, that is, the total area enclosed by the bond-slip curve; $\tau(s)$ is the interface shear load; S is the maximum interface slip value.

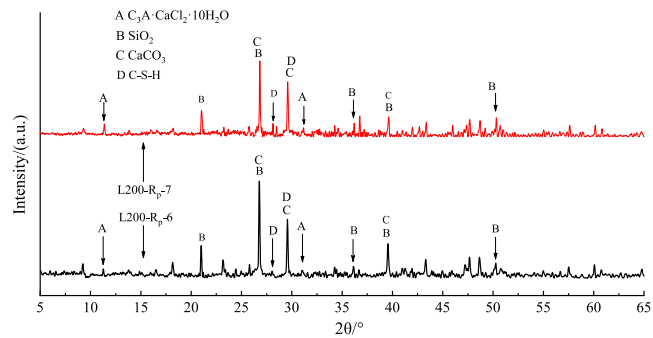
As shown in Fig. 8, in the case of other conditions, the higher the number of dry and wet cycles of chlorine salt, the smaller the interfacial fracture energy is; The interfacial fracture energy of 150 dry and wet cycles is reduced by 67.3% compared with 90 dry and wet cycles, suggesting that an increase of chlorine salt dry–wet circulation interface fractures can have a relatively obvious effect. The interface bonding resists crack instability extension performance degradation, and fracture damage is more likely to occur because of the increasing chlorine salt dry–wet circulation, allowing interfacial microstructure damage degradation to accumulate. The decrease in density of the entire microstructure leads to the destruction of the interfacial bonding properties. As shown in Fig. 8, the interfacial fracture energies of the two groups of specimens with different cyclic frequencies were calculated and compared. We found that a single cycle time significantly increased the interfacial fracture. Using 2 day/time cyclic frequency specimens, its fracture energy was reduced by 42.7% relative to the 1 day/time cycle frequency. Because the dry–wet circulation frequency sodium chloride solution soak time and indoor drying time increased, the effect of dry shrinkage and wet expansion of interface concrete was more obvious, and more cracks and holes reduced the interface bonding performance. Figure 8 shows that as the concentration of sodium chloride interface fracture increased, the interface fracture energy in the 7.5% chlorine salt concentration was 45.5% lower than the 2.5% chlorine salt concentration, which reduces the interface bonding effect. The interface was more prone to bond fracture damage. As shown in the Fig. 8, the increase in bond length of the reinforcement layer is more significant for the increase of interfacial fracture energy, and the interfacial fracture energy in the reinforcement layer bond length is 300 mm compared with the 100 mm increase of 79.5%. Thus, the bond length has a great influence on the interfacial fracture energy. Increasing the interface bond length of the reinforcement layer can greatly improve the interface bonding performance because the interface bond is mainly composed of mechanical bite force and interface friction resistance. As the bond length increases,



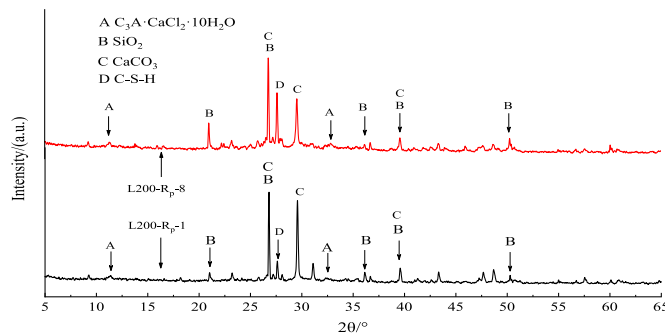
a in different environments



b in different chloride salt concentrations



c in different cycle times



d in different cycle frequencies

Fig. 7 XRD diagrams.

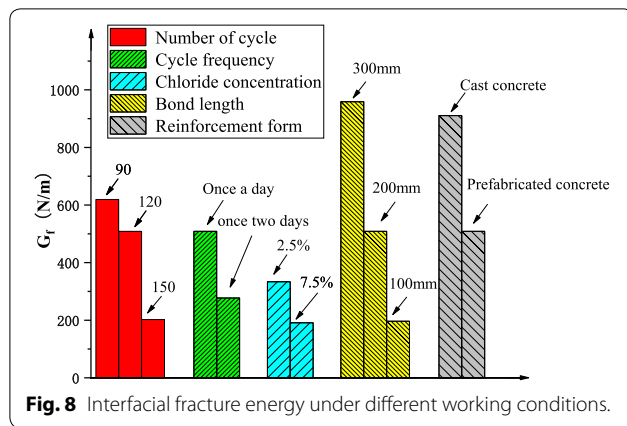


Fig. 8 Interfacial fracture energy under different working conditions.

the interfacial bonding area increases, and the two types of forces increase in the interface. It can be seen from Fig. 8 that the interface fracture energy is reduced by 44.1% when using the prefabricated TRC plate, compared with the cast-in-place reinforcement, and the interface fracture energy is significantly reduced when the prefabricated TRC plate is used for reinforcement. This is because when there is reinforcement of existing concrete, there is a transition zone at the interface. Due to the complexity of the structure of the part, it is the weak position of the whole test piece after reinforcement. When prefabricated TRC plate are used for reinforcement, there are two interfacial transition zones between TRC plate and fine-grained concrete and existing concrete, while in situ reinforcement, there is only one interfacial transition zone between fine-grained concrete and existing concrete. Therefore, when the prefabricated TRC plate is used for reinforcement, the interface is more susceptible to bond failure.

In summary, reducing the concentration of sodium chloride, speeding up the frequency of the wet and dry cycles of chlorine salt, reducing the number of wet and dry cycles of chlorine salt, increasing the bonding length of the strengthened interface and using cast-in-place reinforcement can effectively improve the fracture energy of the interface and improve the overall bonding performance of the interface in the corrosive environment of chlorine salt. Therefore, the interface fracture energy can be used to further analyse the bond performance of existing concrete strengthened by TRC, and the analysis results are in good agreement with the failure mechanism analysis of the interface bond analysed by the microscopic angle.

4 Conclusion

Based on the double-sided shear test, this paper explains the interface bond performance of TRC-reinforced existing concrete from two perspectives, including test results and theoretical analysis, and draws the following conclusions:

- 1) The interface failure modes under chloride erosion are mainly divided into three types of interface failure models: double-sided shear failure, TRC layered failure and existing concrete failure. Among them, double-sided shear failure is the main failure mode, but the interface failure mode can be changed by adopting cast-in-place reinforcement and increasing the bonding length to enhance the interface bonding performance.
- 2) There are few types of interfacial phases in the conventional environment, and the entire microstructure is relatively dense. Under the influence of chlorine salt, a new erosion product, Friedel's salt, was produced in the microscopic substance of the interface. Furthermore, obvious damage and degradation occurred in the microstructure. The whole microstructure was loose and porous, there were acicular and short columnar hydration products in the pores, and obvious cracks were generated.
- 3) The interfacial fracture energy can better characterize the interfacial bond performance under chloride erosion. Studies have found that reducing sodium chloride concentration under chloride erosion, accelerating the frequency of chloride dry and wet cycles, reducing the number of chloride dry and wet cycles, increasing the bonding length of the strengthened interface and using cast-in-place reinforcement can effectively improve the interfacial fracture energy and improve the interfacial bond performance.

Acknowledgements

The authors gratefully acknowledge the financial support from the Jiangsu Provincial Key Research and Development Program (BE2019642). The experimental work described in this paper was conducted at the Jiangsu Key Laboratory of Environmental Impact and Structural Safety in Civil Engineering in the China University of Mining and Technology. Helps during the testing from staffs and students at laboratory are greatly acknowledged.

Authors' contributions

The first author SL mainly undertakes the analysis of data and the writing of the paper. The corresponding and second author SY is mainly responsible for the overall structure and further modification of the paper. The third author YG mainly conduct the collecting of data. All authors read and approved the final manuscript.

Funding

The financial support from the Jiangsu Provincial Key Research and Development Program (BE2019642).

Availability of data and materials

The datasets used or analysed during the current study are available from the corresponding author on reasonable request.

Competing interests

The authors declare that they have no competing interests.

Author details

¹ Jiangsu Key Laboratory of Environmental Impact and Structural Safety in Engineering, School of Mechanics & Civil Engineering, China University of Mining and Technology, Xuzhou 221116, Jiangsu, China. ² State Key Laboratory for Geomechanics & Deep Underground Engineering, China University of Mining and Technology, Xuzhou 221116, Jiangsu, China.

Received: 18 August 2019 Accepted: 10 March 2020

Published online: 04 June 2020

References

- Ascione, L., Felice, G., & Santis, S. (2015). A qualification method for externally bonded Fibre Reinforced Cementitious Matrix (FRCM) strengthening systems. *Composites Part B Engineering*, *78*, 497–506.
- Balonis, M., Lothenbach, B., Saout, G. L., & Glasser, F. P. (2010). Impact of chloride on the mineralogy of hydrated Portland cement systems. *Cement and Concrete Research*, *40*(7), 1009–1022.
- Barhum, R., & Mechtcherine, V. (2012). Effect of short, dispersed glass and carbon fibres on the behaviour of textile-reinforced concrete under tensile loading. *Engineering Fracture Mechanics*, *92*(92), 56–71.
- Bournas, D. A., Lontou, P. V., Papanicolaou, C. G., & Triantafillou, T. C. (2007). Textile-reinforced mortar versus fiber-reinforced polymer confinement in reinforced concrete columns. *ACI Structural Journal*, *104*(6), 740–748.
- D'Ambrisi, A., Feo, L., & Focacci, F. (2012). Bond-slip relations for PBO-FRCM materials externally bonded to concrete. *Composites: Part B*, *43*(8), 2938–2949.
- D'Ambrisi, A., Feo, L., & Focacci, F. (2013). Experimental analysis on bond between PBO-FRCM strengthening materials and concrete. *Composites: Part B*, *44*, 524–532.
- Detassis, M., Frydman, E., Vrieling, D., Zhou, X. F., Wagner, H. D., & Nairn, J. A. (1996). Interface toughness in fibre composites by the fragmentation test. *Composites: Part A*, *27*(9), 769–773.
- Diab, A. M., Elmoaty, A. E. M. A., & Eldin, M. R. T. (2017). Slant shear bond strength between self compacting concrete and old concrete. *Construction and Building Materials*, *130*, 73–82.
- Elakneswaran, Y., Nawa, T., & Kurumisawa, K. (2009). Electrokinetic potential of hydrated cement in relation to adsorption of chlorides. *Cement and Concrete Research*, *39*(4), 340–344.
- Hegger, J., Will, N., Bruckermann, O., & Voss, S. (2006). Loading-bearing behavior and simulation of textile-reinforced concrete. *Materials and Structures*, *39*(8), 765–776.
- Li, G., Xie, H., & Xiong, G. (2001). Transition zone studies of new-to-old concrete with different binders. *Cement & Concrete Composites*, *23*(4–5), 381–387.
- Lu, C., Gao, Y., Cui, Z., & Liu, R. (2007). Experimental analysis of chloride penetration into concrete subjected to drying-wetting cycles. *Journal of Materials in Civil Engineering*, *27*(12), 77–86.
- Marinescu, M., & Brouwers, J. (2012). Chloride binding related to hydration products part I: ordinary Portland Cement. *Cement and Concrete Research*, *42*(2), 282–290.
- Momayez, A., Ehsani, M., Ramezani-pour, A., & Rajaie, H. (2005). Comparison of methods for evaluating bond strength between concrete substrate and repair materials. *Cement and Concrete Research*, *35*(4), 748–757.
- Mousa, M. (2015). Factors affecting bond between repairing concrete and concrete substrate. *International Journal of Engineering and Innovative Technology*, *4*(11), 47–56.
- Ortlepp, R., Hampel, U., & Curbach, M. (2006). A new approach for evaluating bond capacity of TRC strengthening. *Cement & Concrete Composites*, *28*, 589–597.
- Peled, A. (2007). Confinement of damaged and non-damaged structural concrete with FRP and TRC sleeves. *Journal of Composites for Construction*, *11*(5), 514–522.
- Triantafillou, T. C., Papanicolaou, C. G., Zissimopoulos, P., & Laourdekis, T. (2006). Concrete confinement with textile-reinforced mortar jackets. *ACI Structural Journal*, *103*(1), 28–37.
- Yang, S., Chen, Y., Du, D., & Fan, G. (2016). Determination of boundary effect on shear fracture energy at steel bar-concrete interface. *Engineering Fracture Mechanics*, *153*, 319–330.
- Yin, S. P., Li, Y., Jin, Z. Y., & Li, P. H. (2018a). Interfacial properties of textile-reinforced concrete and concrete in the chloride freeze-thaw cycle. *ACI Materials Journal*, *115*(2), 197–208.
- Yin, S. P., Xu, S., & Lv, H. (2014). Flexural behavior of reinforced concrete beams with TRC tension zone cover. *Journal of Materials in Civil Engineering*, *26*(2), 320–330.
- Yin, S. P., Xu, S., & Wang, F. (2015). Investigation on the flexural behavior of concrete members reinforced with epoxy resin-impregnated textiles. *Materials and Structures*, *48*(1–2), 153–166.
- Yin, S. P., Zhao, L., & Li, P. H. (2018b). Failure model of bond force between TRC and old concrete. *Journal of Hunan University (Natural Sciences)*, *45*(01), 77–83. (in Chinese).

Publisher's Note

Springer Nature remains neutral with regard to jurisdictional claims in published maps and institutional affiliations.

Submit your manuscript to a SpringerOpen® journal and benefit from:

- Convenient online submission
- Rigorous peer review
- Open access: articles freely available online
- High visibility within the field
- Retaining the copyright to your article

Submit your next manuscript at ► [springeropen.com](https://www.springeropen.com)